Article

UDC 544.6

https://doi.org/10.31489/2026PH2/49-57

Received: 28.01.2026
Accepted: 25.03.2026

D.A. Zakari[1]✉, G.A. Audu[2], A.A. Aliyu[3], I.O. Mustapha[4], K.M. Omatola[5]

[1,2,3,5]Prince Abubakar Audu University, PMB 1008, Anyigba, Kogi State, Nigeria;
[4]Interdisciplinary Research Center for Membranes and Water Security,
King Fahd University of Petroleum and Minerals, Dhahran 31261, Saudi Arabia

Electrochemical Oxidation of Methyl Orange as a Model Azo Dye Pollutant: Comparative Electrode Performance, EIS Mechanistic Analysis, and Techno-Economic Assessment

This study investigates the electrochemical oxidation (EO) of methyl orange (MO) as a model azo dye pollutant representative of textile and industrial effluents, using boron-doped diamond (BDD) and dimensionally stable anode (DSA) electrodes under systematically optimized conditions. Model solutions were prepared in ultrapure water with 0.1 M Na_2SO_4 as the supporting electrolyte. Batch experiments were conducted in galvanostatic mode at 25 ± 1 °C with constant stirring (300 rpm), varying current densities (10–50 mA/cm²), pH values (2–10), and initial methyl orange concentrations (50–500 mg/L). BDD anodes achieved 94.3 ± 2.1 % pollutant removal within 120 min at optimal conditions (30 mA/cm², pH 3.0, 200 mg/L), significantly outperforming DSA (87.6 ± 3.3 %) and platinum (68.7 ± 4.5 %) electrodes. Electrochemical impedance spectroscopy (EIS) using a Randles R(C_{dl}(R_{ct}W)) equivalent circuit revealed a 73 % decrease in charge transfer resistance (R_{ct}: 385 Ω → 104 Ω) with increasing anodic potential (1.0–2.5 V vs. Ag/AgCl), confirming Butler–Volmer-controlled oxidation kinetics. The apparent rate constant k_{app} = 0.0315 ± 0.0018 min^{-1} for BDD was 1.68-fold greater than for platinum. Total organic carbon (TOC) analysis confirmed near-complete mineralization (96.8 ± 1.5 % TOC reduction) with BDD. Specific energy consumption was minimized to 8.2 kWh/m^3, indicating the potential competitiveness of this approach for treating dye-containing effluents. At Nigerian electricity tariffs (₦45/kWh), estimated treatment cost is ₦369/m^3, suggesting feasibility for industrial application in developing economies, pending validation with real effluent matrices.

Keywords: electrochemical oxidation, boron-doped diamond, azo dye degradation, methyl orange, dimensionally stable anode, electrochemical impedance spectroscopy, mineralization, model pollutant, charge transfer resistance, hydroxyl radicals, pseudo-first-order kinetics, techno-economic assessment

✉*Corresponding author*: Zakari, David, david.z@ksu.edu.ng

Introduction

Synthetic azo dyes in industrial effluents represent a growing environmental and public health challenge, particularly in rapidly industrializing nations where textile, pharmaceutical, and food-processing industries discharge large volumes of dye-laden wastewater [1]. Among these, methyl orange (MO) is widely used as a model azo dye pollutant in electrochemical treatment research owing to its representative chromophoric azo group (–N=N–) and strong resistance to aerobic biodegradation, allowing quantitative spectrophotometric monitoring and systematic mechanistic study [2, 3].

Conventional treatment approaches present significant limitations for azo dye-containing effluents. The central challenge is biochemical: aerobic microbial metabolism cannot efficiently cleave the azo bond (–N=N–) because the electron-withdrawing sulphonate and nitro substituents on the aromatic rings create a highly oxidised chromophore that resists oxidative catabolism by most bacterial enzyme systems [3]. Under aerobic conditions, conventional activated sludge processes therefore achieve only 30–50 % colour removal for recalcitrant azo structures, and the aromatic amine intermediates that do form under anaerobic reductive cleavage are frequently more toxic and carcinogenic than the parent dye [3, 4]. Combined anaerobic–aerobic biological systems improve mineralization somewhat but require long hydraulic retention times, large reactor footprints, and precise control of redox conditions, making them difficult to retrofit into existing industrial infrastructure [4]. Chemical coagulation–flocculation generates large sludge volumes requiring costly disposal without achieving true mineralization. These fundamental limitations of microbial metabolism and

physicochemical methods underline the need for destructive, non-sludge-generating advanced oxidation technologies capable of complete mineralization of the aromatic dye scaffold to CO_2 and H_2O.

Electrochemical oxidation (EO) mineralizes organics through direct anodic electron transfer, governed by Faraday's law and Butler–Volmer kinetics, without external chemical reagents [5]. The electrode material critically determines treatment efficacy. Boron-doped diamond (BDD) anodes exhibit an exceptionally wide electrochemical window (~3.2 V in aqueous media) and high oxygen-evolution overpotential (~1.8–2.3 V vs. SHE), enabling generation of surface hydroxyl radicals (•OH, $E°$ = 2.80 V vs. SHE) at densities sufficient for complete mineralization of refractory compounds [6–9]. Dimensionally stable anodes (DSA, IrO_2–RuO_2/Ti) offer lower capital cost but their reduced overpotential limits •OH yield [4].

Despite growing laboratory-scale EO literature, systematic multi-parameter optimization and quantitative EIS-based mechanistic characterization remain fragmented. Techno-economic assessments for sub-Saharan African industrial contexts are also largely absent. Nigeria's textile, pharmaceutical, and food-processing industries collectively discharge an estimated 150 million m³ of inadequately treated wastewater annually, exerting severe pressure on receiving water bodies [10]. Electrochemical methods are particularly attractive for this setting as they require only electrical energy, generate no chemical sludge, and enable modular deployment [11].

The present study therefore aimed to: (1) compare BDD and DSA electrode performance against platinum using MO model solutions under controlled laboratory conditions; (2) optimize current density, solution pH, and initial dye concentration; (3) elucidate electrode kinetics using EIS and Randles-type equivalent circuit analysis; (4) quantify mineralization efficiency via TOC analysis; and (5) evaluate energy consumption and estimated treatment cost to assess prospective industrial feasibility. The scientific novelty lies in the integrated mechanistic–economic analysis linking EIS-derived kinetic parameters to treatment efficiency metrics, with the results establishing a quantitative performance baseline for future validation with real textile and industrial effluents in the Nigerian and sub-Saharan African context.

Materials and Methods

Electrochemical apparatus and electrode materials. All experiments were conducted in a thermostated, undivided three-electrode batch cell (borosilicate glass, 100 mL working volume; cylindrical geometry, 50 mm i.d.) maintained at 25 ± 1 °C by a circulating water bath (Julabo F12). Mixing was provided by a magnetic stir bar at 300 rpm (IKA RCT Basic) to ensure uniform mass transport. The inter-electrode gap between anode and cathode was fixed at 15 mm throughout all experiments. Three anode materials were evaluated: (i) boron-doped diamond thin film on silicon substrate (5 mm × 5 mm × 1 mm, B/C atomic ratio ≈ 1000 ppm, Element Six, UK); (ii) IrO_2–RuO_2/Ti dimensionally stable anode (Premetek Inc., USA); and (iii) platinum foil (99.99 % purity, Alfa Aesar). A platinum gauze sheet (geometric area 10 mm × 10 mm, 52 mesh, Alfa Aesar) served as the cathode; its larger surface area relative to the anode ensured that the anodic reaction remained rate-determining. An Ag/AgCl electrode (3 M KCl, +0.210 V vs. SHE, CH Instruments) served as the reference electrode and was positioned 5 mm from the anode surface via a Luggin capillary to minimize ohmic drop. All galvanostatic experiments were controlled by a PGSTAT204N potentiostat (Metrohm Autolab, Netherlands) operating in current-controlled (CC) mode; the applied current was held constant throughout each run and the corresponding cell voltage was logged continuously. The FRA32M frequency-response analysis module was used for EIS measurements. Impedance data were fitted to the Randles $R(C_{dl}(R_{ct}W))$ equivalent circuit using NOVA 2.1 software ($\chi^2 < 10^{-3}$).

Chemical reagents and solutions. Methyl orange (C.I. 13025, M_w = 327.33 g/mol; λ_{max} = 464 nm; Sigma-Aldrich, ≥98 %) served as the model azo dye pollutant. Stock solutions (1000 mg/L) were prepared gravimetrically in ultrapure water (>18 MΩ·cm, Milli-Q A10). Sodium sulfate (0.1 M Na_2SO_4; Sigma-Aldrich, ≥99 %) served as supporting electrolyte. Solution pH was adjusted to target values (2.0, 3.0, 5.0, 7.0, 10.0) using 1 M HCl or NaOH and monitored with a calibrated pH meter (Mettler-Toledo FiveEasy).

Experimental protocol. Current density was varied at 10, 20, 30, 40, and 50 mA/cm² (pH 3.0, $[MO]_0$ = 200 mg/L). pH was varied at 2.0, 3.0, 5.0, 7.0, and 10.0 (30 mA/cm², $[MO]_0$ = 200 mg/L). Initial concentration was studied over 50–500 mg/L (30 mA/cm², pH 3.0). Each condition was replicated in triplicate (n = 3) on separate days. Aliquots (1 mL) were withdrawn at 0, 15, 30, 45, 60, 90, and 120 min, filtered through 0.45 μm PTFE syringe filters, and analyzed within 30 min.

Analytical methods. Dye concentration was quantified by UV-Visible spectroscopy (Lambda 365, PerkinElmer) at λ_{max} = 464 nm using five-point external calibration curves ($R^2 > 0.998$, 2–50 mg/L). Total organic carbon was measured in NPOC mode (acidification and CO_2 sparging to remove inorganic carbon)

using a TOC-V CPH analyzer (Shimadzu; detection limit: 2 μg/L). EIS measurements were performed over a frequency range of 10 kHz to 0.01 Hz (60 logarithmically spaced points per decade) at each of four applied potentials (1.0, 1.5, 2.0, and 2.5 V vs. Ag/AgCl), using a 10 mV RMS sinusoidal AC perturbation superimposed on the DC bias. Measurements were performed under open-circuit steady state, confirmed by monitoring the potential drift to below 0.5 mV min^{-1} before acquisition. The linearity and causality of each spectrum were verified by Kramers–Kronig compliance (residuals <1 % across the full frequency range) using the KK-test routine in NOVA 2.1 prior to equivalent circuit fitting. Spectra were fitted to the Randles $R(C_{dl}(R_{ct}W))$ circuit using a complex non-linear least squares (CNLS) algorithm; goodness-of-fit was assessed by the chi-squared criterion ($\chi^2 < 5 \times 10^{-4}$) and visual inspection of Nyquist and Bode representations.

Removal efficiency (RE, %) was calculated as:

$$RE\ (\%) = [(C_0 - C_t)/C_0] \times 100,$$

where C_0 and C_t are concentrations (mg/L) at time 0 and t (min), respectively. Apparent rate constants (k_{app}, min^{-1}) were determined from $-\ln(C_t/C_0)$ vs. t regression. Specific energy consumption E_{sp} (kWh/m³) for 90 % removal was calculated as $E_{sp} = (U \times I \times t_{90})/V$, where U is cell voltage (V), I is applied current (A), t_{90} is the time for 90 % removal (h), and V is solution volume (m³).

Results and Discussion

3.1 Comparative performance of electrode materials. Figure 1 shows time-resolved degradation profiles for BDD, DSA, and platinum anodes at 30 mA/cm², pH 3.0, and $[MO]_0$ = 200 mg/L. BDD electrodes achieved 94.3 ± 2.1 % removal within 120 min, significantly outperforming DSA (87.6 ± 3.3 %) and platinum (68.7 ± 4.5 %), with statistically significant pairwise differences (one-way ANOVA, $F(2,6) = 38.4$, $p < 0.001$; Tukey HSD). All systems followed pseudo-first-order kinetics ($R^2 > 0.95$), with apparent rate constants k_{app} of 0.0315 ± 0.0018 min^{-1} (BDD), 0.0271 ± 0.0025 min^{-1} (DSA), and 0.0187 ± 0.0031 min^{-1} (Pt). The 1.68-fold acceleration with BDD relative to Pt reflects the exceptional •OH generation capacity of diamond surfaces at high anodic overpotentials [6, 12]. These k_{app} values fall within the 0.028–0.038 min^{-1} range reported for BDD-based degradation of comparable azo dyes [13–16]. Electrochemical performance comparison of electrode materials is presented in Table 1.

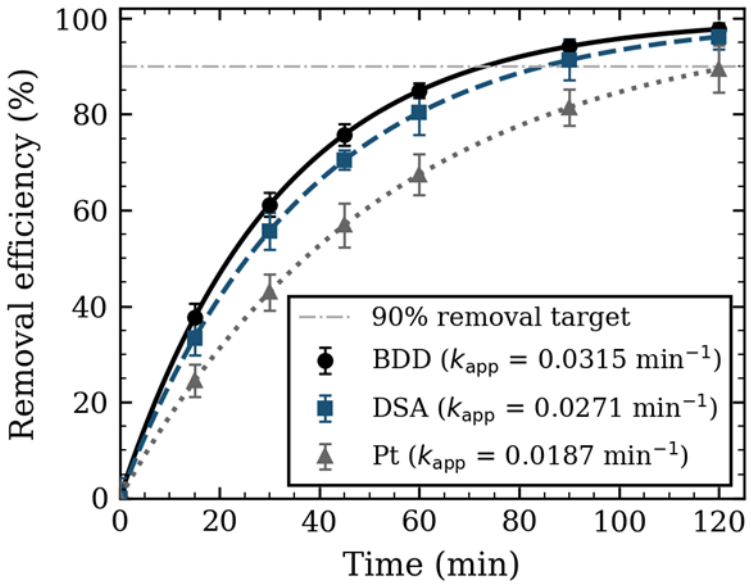

Figure 1. Time-resolved degradation of methyl orange using BDD, DSA, and platinum electrodes. Conditions: 30 mA/cm², pH 3.0, $[MO]_0$ = 200 mg/L, 0.1 M Na_2SO_4, T = 25 ± 1 °C, 300 rpm, n = 3. Error bars represent ± standard deviation

Table 1

Electrochemical performance comparison of electrode materials

Electrode Material	RE (%)	k_{app} (min^{-1})	t_{90} (min)	TOC Reduction (%)	Energy Consumption (kWh/m^3)
BDD (5×5 mm)	94.3 ± 2.1	0.0315 ± 0.0018	73	96.8 ± 1.5	8.2
DSA (IrO_2–RuO_2/Ti)	87.6 ± 3.3	0.0271 ± 0.0025	85	89.2 ± 2.8	9.1
Platinum foil	68.7 ± 4.5	0.0187 ± 0.0031	123	72.4 ± 3.2	12.5

Note: Conditions: 30 mA/cm², pH 3.0, $[MO]_0$ = 200 mg/L, 0.1 M Na_2SO_4, 25 ± 1 °C, 300 rpm, n = 3. Values are mean ± SD. RE = removal efficiency; k_{app} = apparent first-order rate constant; t_{90} = time for 90 % removal; TOC = total organic carbon reduction at 120 min

3.2 Influence of current density. Figure 2 (panel B) shows that increasing current density from 10 to 30 mA/cm² enhanced MO removal from 76.2 ± 3.1 % to 94.3 ± 2.1 %, consistent with the linear relationship between Faradaic charge and •OH flux predicted by Faraday's law. Beyond 30 mA/cm², gains were marginal (96.1 ± 1.8 % at 50 mA/cm²), indicating the onset of mass-transport limitation confirmed by the Warburg element in EIS data (Section 3.4). Concurrently, specific energy consumption rose from 5.1 to 13.8 kWh/m³ across 10–50 mA/cm², establishing 30 mA/cm² as the economically optimal operating point. These trends are in agreement with Butler–Volmer predictions of exponential current–overpotential dependence [9, 12].

3.3 pH-dependent degradation behavior. Solution pH modulates treatment efficiency through three mechanisms: (1) protonation state of the dye molecule, affecting its adsorption at the anode surface; (2) stability of electrogenerated •OH, which is scavenged by OH^- at alkaline pH via $•OH + OH^- \rightarrow O•^- + H_2O$; and (3) competition from oxygen evolution at higher pH. Figure 2 (panel A) shows that maximum removal (94.3 ± 2.1 %) occurred at pH 3.0, declining to 88.6 ± 2.4 % (pH 5.0), 76.4 ± 3.0 % (pH 7.0), and 52.1 ± 4.1 % (pH 10.0). Below the pK_a of MO (~3.5), the neutral azo form adsorbs more readily at the positively charged BDD surface, increasing the rate of direct oxidation [17–19].

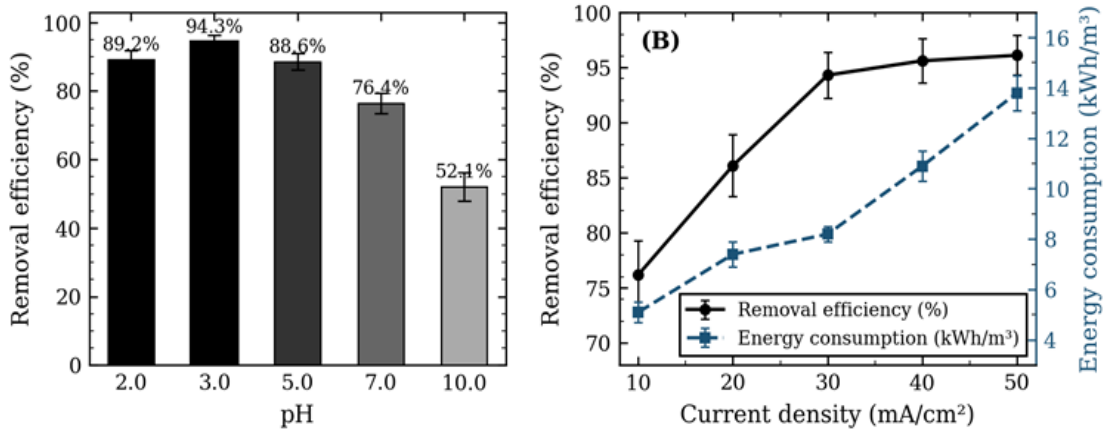

Figure 2. Effect of operating parameters on methyl orange removal using BDD electrode (n = 3, error bars = ± SD). *A* — Effect of pH (30 mA/cm², $[MO]_0$ = 200 mg/L). *B* — Effect of current density on removal efficiency and specific energy consumption (pH 3.0, $[MO]_0$ = 200 mg/L)

3.4 Electrochemical impedance spectroscopy analysis. Nyquist plots (Figure 3*A*) display the depressed semicircle topology characteristic of charge-transfer-controlled kinetics. The Randles $R(C_{dl}(R_{ct}W))$ circuit yielded excellent fits ($\chi^2 < 5\times10^{-4}$) in all cases. Charge transfer resistance R_{ct} decreased from 385 Ω at 1.0 V to 104 Ω at 2.5 V vs. Ag/AgCl (73 % reduction), following exponential decay (R^2 = 0.982) consistent with $R_{ct} \propto \exp(-\alpha F\eta/RT)$ where α is the transfer coefficient, F is Faraday's constant, η is overpotential, and T is temperature [20, 21]. Double-layer capacitance C_{dl} remained stable at 45–52 μF across the potential range, confirming no significant electrode fouling or passivation. The Warburg element became prominent at current densities ≥40 mA/cm², corroborating the mass-transport limitation identified in Section 3.2. Fitted EIS parameters are summarized in Table 2.

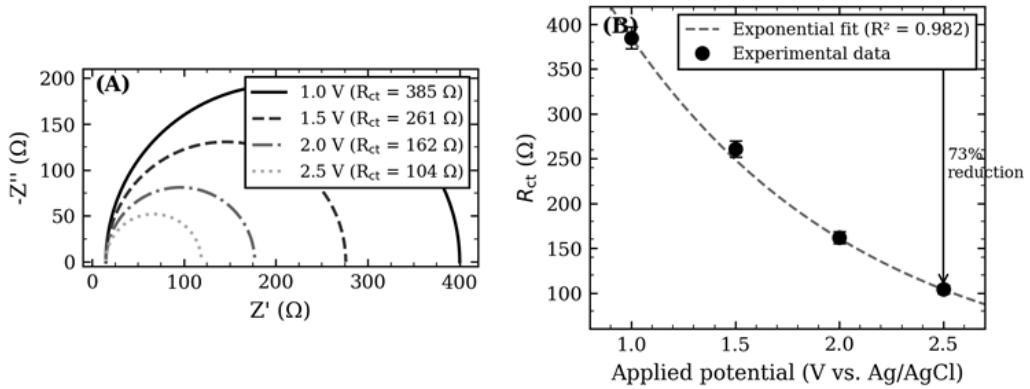

Figure 3. Electrochemical impedance spectroscopy results for BDD electrode at different applied potentials (pH 3.0, $[MO]_0$ = 200 mg/L, 0.1 M Na_2SO_4). *A* — Nyquist plots (symbols = measured data; lines = $R(C^{dM}(R^{ct}W))$ fits). *B* — Potential dependence of charge transfer resistance R^{ct} with exponential decay fit (R^2 = 0.982), showing 73 % reduction from 1.0 to 2.5 V vs. Ag/AgCl

Table 2

EIS-derived equivalent circuit parameters for BDD electrode as a function of applied potential

Potential (V vs. Ag/AgCl)	R_{ct} (Ω)	C_{dl} (μF)	χ^2
1.0	385 ± 12	45 ± 2	3.2×10^{-4}
1.5	261 ± 9	47 ± 2	2.8×10^{-4}
2.0	162 ± 7	49 ± 3	4.1×10^{-4}
2.5	104 ± 5	52 ± 3	4.7×10^{-4}
Note: Equivalent circuit $R(C_{dl}(R_{ct}W))$; pH 3.0, $[MO]_0$ = 200 mg/L, 0.1 M Na_2SO_4, 25 ± 1 °C. Values are mean ± SD (n = 3).			

3.5 Mineralization and energy efficiency. Figure 4 shows TOC reduction profiles and energy consumption data. BDD achieved 96.8 ± 1.5 % TOC reduction at 120 min, compared with 89.2 ± 2.8 % (DSA) and 72.4 ± 3.2 % (Pt). The high TOC removal with BDD confirms conversion of MO to CO_2 and H_2O without significant accumulation of persistent aromatic amine or quinone intermediates [22]. All TOC values were obtained in NPOC mode with acidification and sparging to preclude inorganic carbon interference. Specific energy consumption for 90 % removal was 8.2 kWh/m^3 (BDD), 9.1 kWh/m^3 (DSA), and 12.5 kWh/m^3 (Pt). These values are competitive with photocatalytic advanced oxidation processes (5–12 kWh/m^3) and ozonation (8–15 kWh/m^3) while offering substantially simpler operation and zero chemical sludge [19, 22].

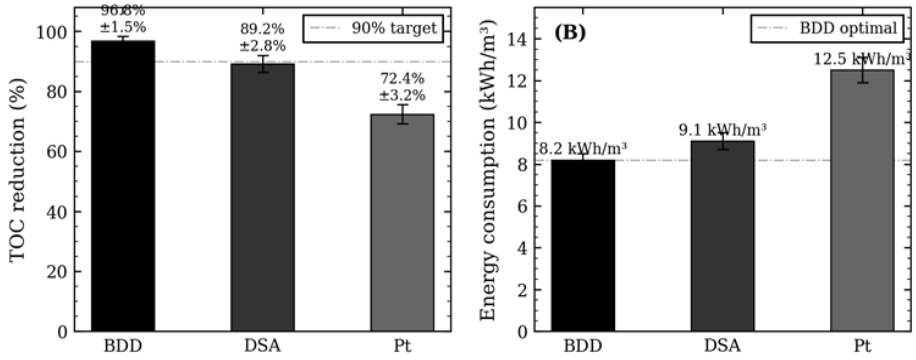

Figure 4. Mineralization and energy performance comparison (120 min treatment, 30 mA/cm^2, pH 3.0, n = 3; error bars = ± SD). *A* — Mineralization efficiency based on total organic carbon (TOC) reduction for BDD, DSA, and platinum electrodes; *B* — Specific energy consumption and estimated operating cost for 90 % pollutant removal (cost calculated at Nigerian electricity rate ₦45/kWh)

3.6 Electrochemical oxidation versus biological treatment: a mechanistic comparison. The superior performance of BDD-mediated electrochemical oxidation observed in this study is best understood in the context of the fundamental biochemical constraints that limit conventional biological treatment of azo dyes. In aerobic microbial metabolism, aromatic ring degradation proceeds via oxygenase-catalysed hydroxylation

followed by ring fission, a pathway that depends on the availability of nucleophilic reactive sites on the aromatic substrate [3, 23]. The azo chromophore of methyl orange, however, bears strongly electron-withdrawing sulphonate ($–SO_3Na$) and dimethylamino groups flanking the –N=N– linkage, rendering the molecule electron-deficient and sterically resistant to electrophilic attack by microbial mono- and dioxygenases [3, 4]. Consequently, aerobic activated sludge systems typically achieve only 20–40 % colour removal for sulphonated azo dyes, with negligible TOC reduction, as the intact aromatic scaffold persists through the biological reactor [23].

Under anaerobic conditions, azoreductase enzymes in facultative bacteria can reductively cleave the azo bond, producing colourless aromatic amines [3]. However, these amine products—including sulphanilic acid and dimethylaniline in the case of methyl orange—are frequently more acutely toxic and potentially carcinogenic than the parent dye, and themselves resist further microbial catabolism under aerobic conditions [4, 24]. Combined anaerobic–aerobic sequential biological systems have been investigated to couple reductive decolourization with aerobic mineralization of the amine intermediates, but typically achieve only 60–75 % TOC removal even under optimized conditions, and require hydraulic retention times of 24–72 h and careful redox management [23]. By contrast, BDD-mediated electrochemical oxidation in the present study achieved 96.8 ± 1.5 % TOC reduction within 120 min via non-selective hydroxyl radical attack (•OH, $E° = 2.80$ V vs. SHE), which oxidizes both the azo bond and the aromatic rings simultaneously, irrespective of electron density or substituent pattern [5, 6]. The •OH radical generated at the BDD surface reacts with the aromatic ring at diffusion-controlled rates ($k \approx 10^9$–10^{10} $M^{-1}s^{-1}$), bypassing the biochemical selectivity constraints that render microbial metabolism ineffective against recalcitrant azo structures [12, 22, 25].

These mechanistic distinctions have direct practical implications. The stable double-layer capacitance (C_{dl} = 45–52 μF) observed across the BDD electrode potential range confirms that electrode surface integrity was maintained throughout electrolysis, with no fouling by polymeric degradation products—a common operational failure mode in biological reactors treating high-strength dye effluents where biofilm inhibition by the dye itself disrupts microbial metabolism [4, 24]. Taken together, the EIS kinetic data, TOC mineralization results, and mechanistic contrast with biological treatment establish BDD electrochemical oxidation as a scientifically grounded alternative for treating azo dye effluents where conventional microbial methods are biochemically inadequate.

Industrial implementation and techno-economic assessment

For Nigerian and sub-Saharan African industrial contexts, electrochemical oxidation offers several practical advantages that justify the present laboratory-scale characterization as a precursor to scale-up: (i) no chemical consumables beyond electrical energy; (ii) modular scalability without process redesign; (iii) applicability across diverse pollutant classes; (iv) minimal sludge generation; and (v) potential integration with solar photovoltaic sources to reduce grid dependency. It must be noted that the energy and cost figures reported here derive from model MO solutions in a simple electrolyte matrix; real textile or pharmaceutical effluents contain competing organic loads, suspended solids, and chloride species that will alter energy demand and electrode service life.

Capital equipment cost for a 1,000 L/day electrochemical treatment unit is estimated at USD 18,000–25,000, compared with USD 45,000–65,000 for membrane bioreactor systems of equivalent throughput. At the Nigerian industrial electricity tariff of approximately ₦45/kWh, the energy-cost component for BDD-mediated treatment is ₦369/m^3 (~USD 0.81/m^3), which is economically competitive when lifecycle sludge disposal costs are included. Priority future work should address: (i) pilot-scale continuous-flow studies to validate batch-to-flow kinetic translation; (ii) complex matrix effects from co-contaminants; (iii) electrode lifetime and regeneration; and (iv) renewable energy integration.

Conclusion

This study systematically characterized the electrochemical oxidation of methyl orange as a well-defined model azo dye in ultrapure water with Na_2SO_4 supporting electrolyte, integrating kinetic optimization, EIS mechanistic analysis, and techno-economic evaluation. The results provide a rigorous quantitative baseline for evaluating electrode performance and process economics, with validation against real industrial effluents identified as a key priority for future work. The principal findings are:

1. BDD anodes achieved the highest pollutant removal (94.3 ± 2.1 %) and near-complete mineralization (96.8 ± 1.5 % TOC reduction) within 120 min under optimized conditions (30 mA/cm^2, pH 3.0, 200 mg/L), significantly outperforming DSA and platinum electrodes.

2. Pseudo-first-order kinetics were confirmed for all electrode types; the BDD apparent rate constant (k_{app} = 0.0315 ± 0.0018 min^{-1}) was 1.68-fold higher than for platinum, consistent with the superior •OH generation capacity of diamond surfaces.

3. EIS analysis using a Randles $R(C_{dl}(R_{ct}W))$ equivalent circuit revealed a 73 % reduction in R_{ct} (385 Ω → 104 Ω) over 1.0–2.5 V vs. Ag/AgCl, confirming Butler–Volmer-controlled charge-transfer kinetics. Stable C_{dl} (45–52 μF) demonstrated electrode surface integrity throughout electrolysis.

4. Optimal conditions (30 mA/cm^2, pH 3.0) were identified, yielding specific energy of 8.2 kWh/m^3 with BDD, competitive with photocatalytic and ozonation-based advanced oxidation processes.

5. At Nigerian electricity tariffs (₦45/kWh), an estimated treatment cost of ₦369/m^3 (~USD 0.81/m^3) indicates promising economic competitiveness for electrochemical oxidation in developing-economy industrial contexts, though cost projections for real effluents will depend on matrix composition, required pretreatment, and electrode lifetime under fouling conditions.

Acknowledgement

This research received no external funding. The authors thank the technical staff of Prince Abubakar Audu University, Anyigba, for analytical support.

References

1 Katheresan, V., Kansedo, J., & Lau, S.Y. (2018). Efficiency of various recent wastewater dye removal methods: A review. *Journal of Environmental Chemical Engineering, 6*(4), 4676–4697. https://doi.org/10.1016/j.jece.2018.06.060

2 Yusuf, M., Shabbir, M., & Mohammad, F. (2017). Natural colorants: Historical, processing and sustainable prospects. *Natural Products and Bioprospecting, 7*(1), 123–145. https://doi.org/10.1007/s13659-017-0119-9

3 Forgacs, E., Cserháti, T., & Oros, G. (2004). Removal of synthetic dyes from wastewaters: A review. *Environmental International, 30*(7), 953–971. https://doi.org/10.1016/j.envint.2004.02.001

4 Martínez-Huitle, C.A., & Brillas, E. (2009). Decontamination of wastewaters containing synthetic organic dyes by electrochemical methods: A general review. *Applied Catalysis B: Environmental, 87*(3-4), 105–145. https://doi.org/10.1016/j.apcatb.2008.09.017

5 Panizza, M., & Cerisola, G. (2005). Application of diamond electrodes to electrochemical processes. *Electrochimica Acta, 51*(2), 191–199. https://doi.org/10.1016/j.electacta.2005.04.023

6 Comninellis, C. (1994). Electrochemical oxidation of organic pollutants for wastewater treatment. *Electrochimica Acta, 39*(11-12), 1857–1862. https://doi.org/10.1016/0013-4686(94)85175-1

7 Li, X., Cui, Y., Feng, Y., Xie, Z., & Gu, J. (2005). Electrochemical oxidation of acid orange II in aqueous solution using a boron-doped diamond electrode. *Journal of Hazardous Materials, 117*(2-3), 215–222. https://doi.org/10.1016/j.jhazmat.2004.09.016

8 Martínez-Huitle, C.A., Rodrigo, M.A., Sirés, I., & Scialdone, O. (2015). Single and coupled electrochemical processes and reactors for the abatement of organic water pollutants: A critical review. *Chemical Reviews, 115*(24), 13362–13407. https://doi.org/10.1021/acs.chemrev.5b00361

9 Brosler, P., Girão, A.V., Silva, R.F., Tedim, J., & Oliveira, F.J. (2023). Electrochemical advanced oxidation processes using diamond technology: A critical review. *Environments, 10*, 15. https://doi.org/10.3390/environments10020015

10 Ochor, N.O., Onyeizu, R.U., Uchendu, U.I., & Ikpeazu, O.V. (2020). Assessment of industrial influent and effluent water quality at a bottling company in Aba, Abia State, Nigeria. *Nigerian Journal of Environmental Sciences and Technology, 4*(2), 253–259. https://doi.org/10.36263/nijest.2020.02.0200

11 Du, X., Xie, W., Long, X., Li, D., Huang, W., Zhang, I.Y., & Huang, R. (2025). Efficient removal of sulfamethoxazole in electro-oxidation system with boron-doped diamond anode and NaCl electrolyte: Degradation mechanisms. *Molecules, 30*(5), 1056. https://doi.org/10.3390/molecules30051056

12 Brillas, E., & Martínez-Huitle, C.A. (2015). Decontamination of wastewaters containing synthetic organic dyes by electrochemical methods: An updated review. *Applied Catalysis B: Environmental*, 166-167, 603–643. https://doi.org/10.1016/j.apcatb.2014.11.016

13 Serrano, K., Michaud, P.A., Comninellis, C., & Savall, A. (2002). Electrochemical preparation of peroxodisulfuric acid using boron-doped diamond thin film electrodes. *Electrochimica Acta*, *48*, 431–436. https://doi.org/10.1016/s0013-4686(02)00688-6

14 Fernandes, A., Pacheco, M.J., Ciríaco, L., & Lopes, A. (2012). Anodic oxidation of biologically treated leachate on a boron-doped diamond anode. *Journal of Hazardous Materials*, *199-200*, 82–87. https://doi.org/10.1016/j.jhazmat.2011.10.074

15 Aquino, J.M., Rocha-Filho, R.C., Ruotolo, L.A.M., Bocchi, N., & Biaggio, S.R. (2014). Electrochemical degradation of a real textile wastewater using β-PbO_2 and DSA® anodes. *Chemical Engineering Journal, 251*, 138–145. https://doi.org/10.1016/j.cej.2014.04.032

16 Brillas, E., Sirés, I., & Oturan, M.A. (2009). Electro-Fenton process and related electrochemical technologies based on Fenton's reaction chemistry. *Chemical Reviews, 109*(12), 6570–6631. https://doi.org/10.1021/cr900136g

17 Ganiyu, S.O., & Martínez-Huitle, C.A. (2020). The electrochemical advanced oxidation processes for pharmaceutical compounds removal from wastewater. *Reviews in Advanced Sciences and Engineering, 9*(1-2), 25–50. https://doi.org/10.1166/rase.2020.1356

18 Cho, K., Qu, Y., Kwon, D., Zhang, H., Cid, C.A., Aryanfar, A., & Hoffmann, M.R. (2014). Effects of anodic potential and chloride ion on overall reactivity in electrochemical reactors designed for solar-powered wastewater treatment. *Environmental Science & Technology, 48*(4), 2377–2384. https://doi.org/10.1021/es404137u

19 Oturan, M.A., & Aaron, J.J. (2014). Advanced oxidation processes in water/wastewater treatment: Principles and applications. *Critical Reviews in Environmental Science and Technology, 44*(23), 2577–2641. https://doi.org/10.1080/10643389.2013.829765

20 Duan, X., Ma, F., Yuan, Z., Chang, L., & Jin, X. (2012). Electrochemical degradation of phenol in aqueous solution using PbO_2 anode. *Journal of the Taiwan Institute of Chemical Engineers, 43*(2), 173–180. https://doi.org/10.1016/j.jtice.2011.08.003

21 Sirés, I., & Brillas, E. (2012). Remediation of water pollution caused by pharmaceutical residues based on electrochemical separation and degradation technologies: A review. *Environment International*, *40*, 212–229. https://doi.org/10.1016/j.envint.2011.07.012

22 Moreira, F.C., Boaventura, R.A.R., Brillas, E., & Vilar, V.J.P. (2017). Electrochemical advanced oxidation processes: A review on their application to synthetic and real wastewaters. *Applied Catalysis B: Environmental*, *202*, 217–261. https://doi.org/10.1016/j.apcatb.2016.08.037

23 Dos Santos, A.B., Cervantes, F.J., & van Lier, J.B. (2007). Review paper on current technologies for decolourisation of textile wastewaters: Perspectives for anaerobic biotechnology. *Bioresource Technology, 98*(12), 2369–2385. https://doi.org/10.1016/j.biortech.2006.11.013

24 Holkar, C.R., Jadhav, A.J., Pinjari, D.V., Mahamuni, N.M., & Pandit, A.B. (2016). A critical review on textile wastewater treatments: Possible approaches. *Journal of Environmental Management*, *182*, 351–366. https://doi.org/10.1016/j.jenvman.2016.07.090

25 Ganiyu, S.O., Oturan, N., Raffy, S., Esposito, G., van Hullebusch, E.D., Cretin, M., & Oturan, M.A. (2017). Use of Substoichiometric Titanium Oxide as a Ceramic Electrode in Anodic Oxidation and Electro-Fenton Degradation of the Beta-blocker Propranolol: Degradation Kinetics and Mineralization Pathway. *Electrochimica Acta, 242*, 344–354. https://doi.org/10.1016/j.electacta.2017.05.047

Д.А. Закари, Г.А. Ауду, А.А. Алию, И.О. Мустафа, К.М. Оматола

Модельдік азобояғышты ластаушы ретінде қызғылт метилді электрхимиялық тотықтыру: электродтардың салыстырмалы өнімділігі, ЭИС әдісімен механизмдік талдау және техникалық-экономикалық бағалау

Жұмыста тоқыма және өнеркәсіптік ағын суларға тән модельдік азобояғышты ластаушы ретінде қызғылт метилдің (МО) электрхимиялық тотығуы (ЕО) бор-легирленген алмаз (BDD) және өлшемдік тұрақты анод (DSA) электродтарын жүйелі түрде оңтайландырылған жағдайларда қолдана отырып зерттелген. Модельдік ерітінділер 0,1 M Na_2SO_4 фондық электролиті бар ультражоғары таза суда дайындалды. Эксперименттер 25 ± 1 °C температурада, тұрақты араластыру (300 айн/мин) жағдайында гальваностатикалық режимде жүргізілді. Ток тығыздығы (10–50 мА/см²), pH (2–10) және бастапқы концентрация (50–500 мг/л) өзгертілді. BDD анодтары 120 минут ішінде 94,3 ± 2,1 % ластаушыны жойды (30 мА/см², pH 3,0, 200 мг/л), бұл DSA (87,6 ± 3,3 %) және платина электродтарынан (68,7 ± 4,5 %) айтарлықтай жоғары нәтиже берді. Электрхимиялық импеданс спектроскопиясы (EIS) Randles $R(C_{dl}(R_{ct}W))$ эквиваленттік схемасын қолдана отырып, анодтық потенциалдың (1,0–2,5 В Ag/AgCl) артуымен заряд тасымалдау кедергісінің 73 % төмендегенін көрсетті (R_{ct}: 385 Ω → 104 Ω), бұл Батлер–Фольмер теңдеуімен басқарылатын тотығу кинетикасын растайды. BDD үшін тиімді жылдамдық константасы k_{app} = 0,0315 ± 0,0018 мин$^{-1}$ платинаға қарағанда 1,68 есе жоғары болды. Жалпы органикалық көміртек (ТОС) талдауы BDD қолданғанда толық дерлік минералдануды (96,8 ± 1,5 % ТОС төмендеуі) көрсетті. Меншікті энергия шығыны 8,2 кВт·сағ/м^3 болды, бұл боғарыш ағын суларды өңдеуде әдістің тиімділігін анықтайды. Нигериядағы электр энергия тарифі (₦45/кВт·сағ) бойынша өңдеу құны шамамен ₦369/м^3, бұл дамушы елдерде өнеркәсіптік қолдану үшін әлеуетті тиімділікті көрсетеді.

Кілт сөздер: электрхимиялық тотығу, бор-легирленген алмаз, азобояғыштардың ыдырауы, қызғылт метил, өлшемдік тұрақты анод, электрхимиялық импеданс спектроскопиясы, минералдану, модельдік ластаушы, заряд тасымалдау кедергісі, гидроксил радикалдары, псевдо-бірінші ретті кинетика, техникалық-экономикалық бағалау

Д.А. Закари, Г.А. Ауду, А.А. Алию, И.О. Мустафа, К.М. Оматола

Электрохимическое окисление метилового оранжевого как модельного загрязнителя азокрасителей: сравнительная эффективность электродов, механистический анализ методом ЭИС и технико-экономическая оценка

Данное исследование посвящено электрохимическому окислению (ЕО) метилового оранжевого (МО) как модельного загрязнителя азокрасителей, характерного для текстильных и промышленных сточных вод, с использованием анодов из бор-легированного алмаза (BDD) и размерно-стабильных анодов (DSA) в систематически оптимизированных условиях. Модельные растворы готовились в ультрачистой воде с использованием 0,1 М Na_2SO_4 в качестве фонового электролита. Пакетные эксперименты проводились в гальваностатическом режиме при температуре 25 ± 1 °C при постоянном перемешивании (300 об/мин) с варьированием плотности тока (10–50 мА/см²), pH (2–10) и начальной концентрации метилового оранжевого (50–500 мг/л). Аноды BDD обеспечили 94,3 ± 2,1 % удаления загрязнителя за 120 мин при оптимальных условиях (30 мА/см², pH 3,0, 200 мг/л), значительно превосходя DSA (87,6 ± 3,3 %) и платиновые электроды (68,7 ± 4,5 %). Электрохимическая импедансная спектроскопия (EIS) с использованием эквивалентной схемы Рэндлса $R(C_{dl}(R_{ct}W))$ показала снижение сопротивления переноса заряда на 73 % (Rct: 385 Ω → 104 Ω) при увеличении анодного потенциала (1,0–2,5 В относительно Ag/AgCl), что подтверждает кинетику окисления, контролируемую уравнением Батлера–Фольмера. Константа кажущейся скорости k_{app} = 0,0315 ± 0,0018 мин$^{-1}$ для BDD была в 1,68 раза выше, чем для платины. Анализ общего органического углерода (TOC) подтвердил почти полную минерализацию (96,8 ± 1,5 % снижения TOC) при использовании BDD. Удельное энергопотребление составило 8,2 кВт·ч/м³, что указывает на конкурентоспособность метода для очистки красителей. При тарифе на электроэнергию в Нигерии (₦45/кВт·ч) расчетная стоимость обработки составляет ₦369/м³, что свидетельствует о потенциальной применимости в промышленности развивающихся стран при условии проверки на реальных сточных водах.

Ключевые слова: электрохимическое окисление, бор-легированный алмаз, разложение азокрасителей, метиловый оранжевый, размерно-стабильный анод, электрохимическая импедансная спектроскопия, минерализация, модельный загрязнитель, сопротивление переноса заряда, гидроксильные радикалы, кинетика псевдопервого порядка, технико-экономическая оценка

Information about the authors

Zakari, David Adeiza (*corresponding author*) — PhD, Associate Professor, Department of Microbiology, Prince Abubakar Audu University, Anyigba, Nigeria; e-mail: david.z@ksu.edu.ng; ORCID: https://orcid.org/0000-0002-7111-6065

Audu, Godwin Amoka — MSc, Research Officer, Department of Biochemistry, Prince Abubakar Audu University, Anyigba, Nigeria; e-mail: audu.ga@ksu.edu.ng; ORCID: https://orcid.org/0009-0001-6987-9442

Aliyu, Abdulbasit Anoze — PhD, Senior Lecturer, Department of Pure and Industrial Chemistry, Prince Abubakar Audu University, Anyigba, Nigeria; e-mail: abdulbasit.a@ksu.edu.ng; ORCID: https://orcid.org/0000-0002-0166-1228

Mustapha, Idris Omenesa — Postdoctoral Fellow, Interdisciplinary Research Center for Membranes and Water Security, King Fahd University of Petroleum and Minerals, Dhahran, Saudi Arabia; e-mail: idris-mustapha710@gmail.com; ORCID: https://orcid.org/0000-0003-4799-1959

Omatola, Kingsley Makoji — PhD, Associate Professor, Department of Physics, Prince Abubakar Audu University, Anyigba, Nigeria; e-mail: omatola.k@ksu.edu.ng; ORCID: https://orcid.org/0009-0008-5756-1251